

Electronic structure Studies of CeAgSb₂

T. Jeong

Department of Physics, University of California, Davis, California 95616

The electronic band structure of CeAgSb₂ has been calculated using the self-consistent full potential nonorthogonal local orbital minimum basis scheme based on the density functional theory. We investigated the electronic structure with the spin-orbit interaction and on-site Coulomb potential for the Ce-derived 4f orbitals to obtain the correctly ground state of CeAgSb₂.

PACS numbers: 71.10.Hf, 71.18.+y, 72.20.Eh, 75.30.Mb

I. INTRODUCTION

The ternary compounds CeXSb₂ (where X=Au, Ag, Cu, Ni, or Pd) have attracted considerable attention recently because they exhibit a large variety of physical properties such as heavy fermion, Kondo insulating, anisotropic transport and magnetic ordering behavior. The various physical properties depend on the hybridization between f electrons and conduction electrons, which is characterized by a Kondo temperature T_K . With a small hybridization the system exhibits a local magnetic moment and orders magnetically, which can be described by the Ruderman-Kittel-Kasuya-Yosida (RKKY) interaction. By increasing the hybridization, the Kondo effect increases and the ordered magnetic moment decreases gradually. With further increase of the hybridization, the system will go into a heavy fermion or intermediate valence regime.

CeAgSb₂ is a Ce-based Kondo lattice system with low-temperature ferromagnetic ordering. Sologub *et al.* [1] reported this compound has weak ferromagnetic order in polycrystalline samples with a net ferromagnetic moment of 0.15 μ_B /Ce at 5 K. Several different groups investigated the magnetic properties of CeAgSb₂ with conflicting results for the magnetic ground state. [2, 3, 4]. In particular, for single crystal samples, the magnetization of CeAgSb₂ is anisotropic[5]. In this case the magnetization for the magnetic field applied parallel to the c-axis shows a ferromagnetic order with a moment of 0.37 μ_B /Ce above 0.025 T at 2 K. For $H \perp c$, the magnetization increases nearly linearly to 1.2 μ_B /Ce below 30 kOe and then remains nearly constant for higher fields, possibly indicating the presence of a metamagnetic transition. Above 200K, the inverse susceptibility is linear to the Curie-Weiss law giving an effective moment of 2.26 μ_B /Ce. In zero field, the resistivity of CeAgSb₂ increases rapidly from 1.16 $\mu\Omega$ cm at 2K to a maximum of 88.1 $\mu\Omega$ cm at 18.2 K. At 9.7K, a sharp change in the slope of the zero field resistivity is observed, consistent with a loss of spin-disorder scattering associated with the magnetic ordering as well as the possible suppression of the Ce hybridization due to the ferromagnetic ordering. At higher temperatures, the resistivity determines a broad local minimum near 150K. The temperature-dependent resistivity of CeAgSb₂ is typical of a Kondo lattice system. Preliminary inelastic neutron scattering measure-

ments indicate a Kondo temperature T_K between 60 and 80K [4]. The magnetoresistance of CeAgSb₂ is either positive or negative, depending on the temperature and orientation of the applied field. This complexity is due to competing contributions from the Ce hybridization, magnetic ordering, and the electronic structure of the compound. The magnetoresistance of a paramagnet is expected to be negative, since the local moments try to align parallel to the applied field, which essentially reduces the spin disorder scattering as the field is increased.

In order to understand the electronic and magnetic properties of CeAgSb₂, we need the electronic band structure studies based on the density functional theory. In this work, the precise self-consistent full potential local orbital minimum basis band structure scheme (FPLO) are employed to investigate the electronic and magnetic properties of CeAgSb₂ with LDA, LDA+U and fully relativistic schemes. We consider the effect of magnetism on the band structure and compare with experiment.

II. CRYSTAL STRUCTURE

CeAgSb₂ crystallizes in the primitive tetragonal ZrCuSi₂ structure, which consists of Sb-CeSb-Ag-CeSb-Sb layers along [001] direction. This crystal structure is described in detail by Myers *et al.* [5]. It belongs to the P4/nmm space group with Ce occupying the 2c site, Ag the 2a, and Sb the 2b, 2c sites. The sites are given, in units of (a, a, c): Ce(0.25, 0.25, 0.26), Ag(0.75, 0.25, 0.5), Sb(0.25, 0.25, 0.84), Sb(0.75, 0.25, 0). We used experimental lattice constants, a= 4.36 Å and c=10.41 Å, in the calculation described below. There are two formula units in the primitive cell.

III. METHOD OF CALCULATIONS

We have applied the full-potential nonorthogonal local-orbital minimum-basis (FPLO) scheme within the local density approximation (LDA).[6] In these scalar relativistic calculations we used the exchange and correlation potential of Perdew and Wang.[7] Ce 4s, 4p, 3d, Ag 5s, 5p, 4d and Sb 4s, 4p states were included as valence states. All lower states were treated as core states. We included the relatively extended semicore 4s, 4p, 4d, 4f, 5s, 5p states

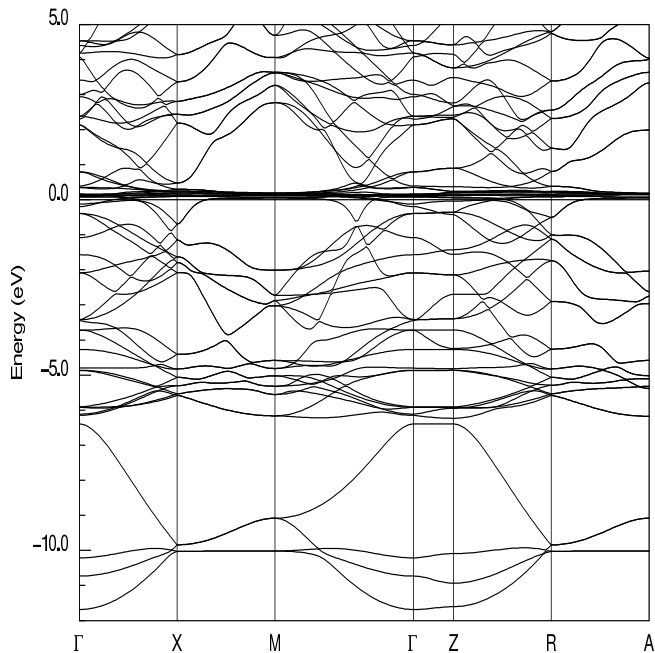


FIG. 1: The full LDA nonmagnetic band structure of CeAgSb_2 along the symmetry lines.

of Ce and 4s, 4p states of Sn and Ag as band states because of the considerable overlap of these states on nearest neighbors. This overlap would be otherwise neglected in our FPLO scheme. Ce 6p states were added to increase the quality of the basis set. The spatial extension of the basis orbitals, controlled by a confining potential $(r/r_0)^4$, was optimized to minimize the total energy. The self-consistent potentials were carried out on a k mesh of 18 k points in each direction of the Brillouin zone, which corresponds to 550 k points in the irreducible zone. A careful sampling of the Brillouin zone is necessitated by the fine structures in the density of states near Fermi level E_F .

IV. RESULTS AND DISCUSSION

We first show the full band structures of CeAgSb_2 within LDA scheme in Fig. 1. The Sb 5s bands lie between -11.5eV and -6.5eV. Between -6.5 and the Fermi level there are of mixed Sb 5p and Ag 4d states. Those very flat bands near the Fermi level are mainly the Ce-centered 4f characters. A prominent feature of the band structure near E_F , besides the 4f bands, is the Ce 5d character which hybridizes with the Ce 4f bands. We also study the on-site atomic-like correlation effects beyond LDA by using LDA+U approach in a rotationally invariant, full potential implementation[8]. Minimizing the LDA+U total energy functional with spin-orbit coupling(SOC) treated self-consistently [9] generates not only the ground state energy and spin densities, but also effective one-electron states and energies that provides the orbital contribution to the moment and Fermi surfaces. The basic difference of LDA+U calculations from

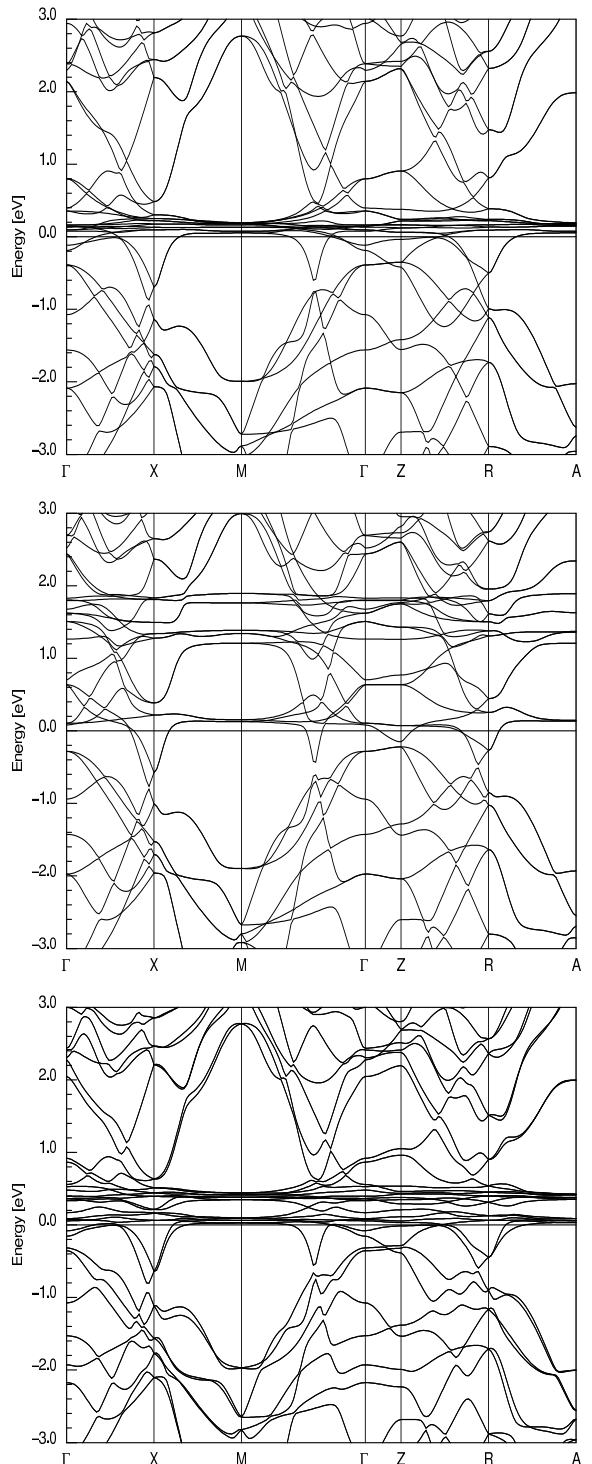


FIG. 2: Top panel: The LDA band structure of CeAgSb_2 along symmetry lines. The very flat bands near the Fermi level are the Ce 4f bands. Middle panel: The band structure within the LDA+U scheme showing that the 4f bands are split in a 1-3-3 fashion from bottom up. Bottom panel: The fully relativistic band structure of CeAgSb_2 showing that spin-orbit coupling splits the 4f states into two manifolds.

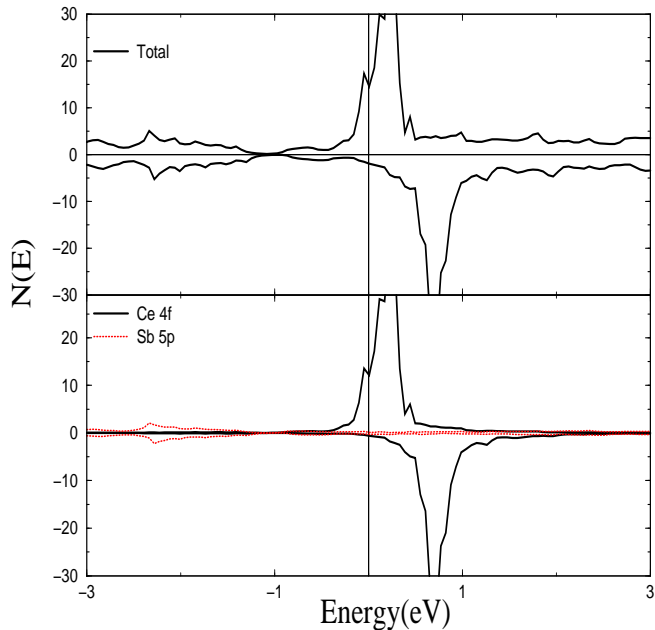


FIG. 3: Projected density of states of CeAgSb_2 . Top panel: total, plotted positively for majority, negatively for minority. Bottom panel: projection of the Ce 4f and Sb 5p, showing that Ce 4f character dominates the states near the Fermi level.

the LDA is its explicit dependence on the on-site spin and orbitally resolved occupation matrices. The Coulomb potential U and the exchange coupling J for the Ce 4f orbitals have been chosen to be 7.5 and 0.68 eV respectively. The resulting band structure calculated within the LDA+ U scheme is shown in middle panel of Fig. 2. We observe that the crystal field splittings of Ce 4f bands within LDA are quite small and in fact difficult to identify due to hybridization with itinerant bands. From LDA+ U , the 4f bands are still very flat but are split (in a 1-3-3 fashion from bottom up) by some combination of the crystal field and the anisotropy of the U interaction by a total 1.6 eV. We also calculated fully relativistic band structure to see the spin-orbit coupling effects, which is shown in the lower panel of Fig. 2. As expected spin-orbit coupling splits the 4f states into two manifolds, located 0.4 eV and 0.05 eV above the Fermi level, the $4f_{7/2}$ and the $4f_{5/2}$ multiplet respectively.

The atom and symmetry projected densities of states (PDOS) shown in Fig.3 clarify the characters of the bands. Because only the DOS distribution near the Fermi level determines the magnetic properties, we concentrate our attention upon the DOS in the vicinity of the Fermi level. At this range, the valence states for Ce or Sb atoms are dominated by 4f and 5p electrons, respectively, and the contributions from other electrons are negligibly small. Because of hybridization, they distribute in a wide

energy range and extend to the unoccupied states, above the Fermi level. These states remain almost unchanged when the spin-orbital interaction or on-site correlation potential are taken into consideration. So only the DOS obtained by LDA calculation for Ce-4f and Sb-5p have been plotted. From the Fig. 3, it can be found that within the LDA calculation, the DOS at the Fermi level are larger and they are mainly of Ce-derived 4f states. The contribution from Ag-derived 4d or Sb-derived 5p states is smaller. When the spin-orbital coupling along the axis (0 0 1) is taken into account, the 4f orbitals are slightly modified. The spin 4f states become wider and the energy shift between centers becomes larger. This is due to the partial splitting between the degenerate 4f states.

Band calculation with the LDA framework cannot yield correctly magnetic moment for many Ce compounds because of the strong correlation interaction between f orbitals. The spin-orbit interaction in these systems is sometimes large and the orbital contribution to magnetic moment cannot be neglected. The calculated magnetic moment of CeAgSb_2 within LDA scheme is $0.61 \mu_B/\text{Ce}$. It is mainly from the Ce-derived 4f orbitals, while almost no contribution from Ag. This is in agreement with the fact that the transition metal T, except Mn, does not carry magnetic moment in CeTSb_2 compounds. When the on-site correlation potential is added to the Ce 4f electron, the degeneracy between the different f orbitals would be lifted and the Hund's rules dominate the locally occupied 4f electrons, which yields the total magnetic moment $0.54 \mu_B/\text{Ce}$. With fully relativistic scheme we calculated the magnetic moment of the value $0.55 \mu_B/\text{Ce}$. As mentioned above, several groups reported the experimental studies on the magnetic moments which do not agree with another, so further experimental investigations are required.

Density functional calculations are very reliable in calculating the instability to ferromagnetism. The presence of an electronic instability is signaled by a divergence of the corresponding susceptibility. In the following we study the uniform magnetic susceptibility using the method of Janak [10]. The uniform magnetic susceptibility of a metal can be written as

$$\chi = \frac{\chi_0}{1 - N(E_F)I}, \quad (1)$$

where the numerator stands for the Pauli susceptibility of a gas of non-interacting electrons proportional to the density of states at the Fermi level $N(E_F)$, and the denominator represents the enhancement due to electron-electron interaction. Within the Kohn-Sham formalism of density functional theory the Stoner parameter I is related to the second derivative of the exchange-correlation functional with respect to the magnetization density. We have evaluated, within the density functional theory formalism, the Stoner enhancement of the susceptibility $\chi = \frac{\chi_0}{1 - IN(E_F)} \equiv S\chi_0$, where $\chi_0 = 2\mu_B^2 N(E_F)$ is the

non-interacting susceptibility and S gives the electron-electron enhancement in terms of the Stoner constant I . We have calculated I using both the Janak-Vosko-Perdew theory [10] and fixed spin moment calculations[11]. The calculated density of states and Stoner parameter normalized per are $N(E_F)=5.8$ states/eV and $I=0.19$ eV. This gives $IN(E_F) = 1.1$, larger than unity, corresponding to a ferromagnetic instability.

Heavy fermion compound is characterized by a larger electronic specific heat coefficient γ . CeAgSb₂ is a moderate heavy fermion compound with $\gamma = 65$ mJ/K²mol[12]. The large specific heat coefficient of CeAgSb₂ compound could not be yielded by our band calculation. This can be seen from the calculated electronic structure. It can be found that the total number of DOS at the Fermi level is about 5.8 states/eV, which corresponds $\gamma_b = 13.6$ mJ/K²mol and underestimate the experiment value by a factor of 4.8. The discrepancy between the band calculation and experiment for specific heat coefficient is attributed to the formation of quasiparticle. There is exchange interaction J between the local f and the conduction electrons in CeAgSb₂. The ground state of Ce compound is determined by the competition of the Kondo and indirect RKKY interaction. With a large J , the Kondo coupling becomes strong and the system located at the borderline of magnetic-nonmagnetic transition. The exchanging interaction between the local f electron and the conduction electrons will result in the formation of quasiparticle. It has a larger mass compared with bare electron and the enhancement of mass increases with the increase of exchanging. Because of the volume contraction, the exchange interaction between the f and the conduction electrons is large in CeAgSb₂. This will re-

sult in the f electrons to behave like itinerant electrons and the narrow f bands to be located at the Fermi level. On the other hand, when the exchanging interaction between f and conduction electrons is smaller, the occupied $4f$ orbitals are located near the Fermi level while the unoccupied $4f$ orbitals are at the conduction bands. The quasiparticle mass is appropriate to the number of DOS at the Fermi level. So the quasiparticle mass is largely enhanced in CeAgSb₂. Indeed, it has been shown that when the Ce $4f$ electrons in CeAgSb₂ are treated as localized electrons, the quasiparticle mass was only enhanced over the band calculation by a factor 4.8.

V. SUMMARY

In this article we showed the results of three different electronic band structure calculations. It shows that the Coulomb potential on Ce $4f$ orbitals and spin-orbit interaction is a key factor to understand the electronic and magnetic properties of CeAgSb₂. When the Coulomb potential is added to the Ce $4f$ orbitals, the degeneracy between the different f orbits would be lifted and they are split into lower Hubbard bands at the Fermi level and unoccupied upper Hubbard bands in the conduction band. The exchange interaction between local f electrons and conduction electrons play an important role in the heavy fermion characters of them. And the fully relativistic band structure scheme shows that spin-orbit coupling splits the $4f$ states into two manifolds, the $4f_{7/2}$ and the $4f_{5/2}$ multiplet.

-
- [1] O.Sologub, H.Noel, A.Leithe-Jasper, P.Rogl, and O.I.Bodak, J. Solid. State Chem. **115**,441 (1995)
- [2] T.Takeuchi, A.Thamizhavel, T.Okubo, M.Yamada, N.Nakamura, T.Yamanoto, Y.Inada, K.Sugiyama, A.Galatanu, E.Yamamoto, K.Kindo, T.Ebihara, and Y. Onuki, Phys. Rev. B **67**, 064403 (2003)
- [3] M.Houshiar, D.T.Adroja, and B.D.Rainford, J.Magn. Mater. **140-144**, 1231, (1995)
- [4] M.J.Thornton, J.G.M.Armitage, G.J.Tomka, P.C.Riedi, R.H.Mitchel, M.Houshiar, D.T.Adroja, B.D.Rainford, and D.Fort, J.Phys: Condens. Matter **10**, 9485 (1998) **59**, 1743 (1999)
- [5] K.D.Myers, S.L.Bud'ko, I.R.Fisher, Z.Islam, H.Kleinke, A.H.Lacerda, and P.C.Canfield, J. Magn. Mater. **205**, 27 (1999)
- [6] K. Koepernik, and H. Eschrig, Phys. Rev. B **59**, 1743 (1999); H.Eschrig, Optimized LCAO Method and the electronic Structure of Extended Systems (Springer,Berlin,1989).
- [7] J. P. Perdew, and Y.Wang, Phys. Rev. B **45**, 13244 (1992).
- [8] A.I.Liechtenstein, V.I.Anisimov and J.Zaanen, Phys. Rev. B **52**, R5468 (1995); A.B.Shick, A.I.Liechtenstein, and W.E. Pickett, Phys. Rev. B **60**, 10728 (1999)
- [9] A.B.Shick, D.L.Novikov, and A.J.Freeman, Phys. Rev. B **57**, R14259 (1997).
- [10] J. F. Janak, Phys. Rev. B **16**, 255 (1977); S. H. Vosko and J. P. Perdew, Can. J. Phys. **53**, 1385 (1975)
- [11] K.Schwarz and P.Mohn, J.Phys. F **14**, L129 (1984)
- [12] Y.Inada, A.Thamizhavel, H.Yamagami, T.Takeuchi, Y.Sawai, S,Ikea, H.Shishido, T.Okubo, M.Yamada, K.Sugiyama, N.Nakamura, T.Yamamoto, K.Kindo, T.Ebihara, A.Galatanu, E.Yamamoto, R.Settai, and Y.Onuki, Phils. Mag. B **82**, 1876 (2002)